



## Development of GEM-PA-nanotrap for purification of foot-and-mouth disease virus



Haiwei Cheng<sup>a,b,c,1</sup>, Jin Chen<sup>a,b,c,1</sup>, Zizheng Cai<sup>d</sup>, Luping Du<sup>a,b,c</sup>, Jibo Hou<sup>a,b,c</sup>, Xuwen Qiao<sup>a,b,c,\*</sup>, Qisheng Zheng<sup>a,b,c,\*</sup>

<sup>a</sup> Institute of Veterinary Immunology & Engineering, Jiangsu Academy of Agricultural Sciences, Nanjing 210014, China

<sup>b</sup> National Research Center of Engineering and Technology for Veterinary Biologicals, Ministry of Agriculture, Key Laboratory of Veterinary Biological Engineering and Technology, Jiangsu Academy of Agricultural Sciences, Nanjing 210014, China

<sup>c</sup> Jiangsu Co-innovation Center for Prevention and Control of Important Animal Infectious Diseases and Zoonoses, Yangzhou 225009, China

<sup>d</sup> Nanjing Agricultural University, Nanjing 210095, China

### ARTICLE INFO

#### Article history:

Received 17 December 2018

Received in revised form 20 April 2019

Accepted 24 April 2019

Available online 26 April 2019

#### Keywords:

FMDV

Affinity purification

Gram-positive enhancer matrix particles

Nanobody

Nanotrap

### ABSTRACT

Vaccination is the primary preventative measure against outbreaks of foot-and-mouth disease (FMD). The efficacy of inactivated FMD vaccines is mainly determined by the integrity of foot-and-mouth disease virus (FMDV) particles (referred to as 146S particles), and impurities in the inactivated vaccines could result in side effects. In this study, we developed an effective affinity purification method for the purification of FMDV from cellular lysates, referred to as GEM-PA-nanotrap. To develop the GEM-PA-nanotrap, a nanobody (Nb205) against FMDV vaccine strain O/MYA98/BY/2010 146S particles was selected from a non-immunized library and fused to a peptidoglycan-binding protein anchor (PA). The PA-Nb205 fusion protein was non-covalently coupled to the surface of Gram-positive enhancer matrix (GEM) particles, which were prepared from the non-living, non-genetically modified, Gram-positive, food-grade *Lactococcus lactis* bacteria. The GEM-PA-nanotrap was used to purify FMDV from cellular lysates through a simple incubation and centrifugation step. The FMDV recovery rate was more than 99%, the efficiency of nonviral protein removal was about 98.3%, and the purification process had almost no effect on the integrity and immunogenicity of 146S particles. Therefore, the GEM-PA-nanotrap has potential as an effective method for the recovery and purification of FMDV during the vaccine manufacturing process.

© 2019 Elsevier Ltd. All rights reserved.

### 1. Introduction

Foot-and-mouth disease (FMD) has been classified as an International Epizootic Office list A disease, which is a highly contagious disease of cloven-hoofed animals. Vaccination with inactivated vaccines is one of the primary strategies for preventing the outbreaks and prevalence of FMD. The efficacy of inactivated foot-and-mouth disease virus (FMDV) vaccines is highly dependent on virion integrity [1,2]. The whole virion, with a sedimentation coefficient of 146S, dissociates into smaller subunits, with sedimentation coefficient of 12S, at temperatures above 56 °C or pHs below 6.0 [3,4], resulting in a great reduction in potency [1,5,6]. During the past few years, the quality of inactivated FMDV vaccines has

been improved and cell suspension cultivation has been widely applied to scalable vaccine production. However, crude inactivated vaccines without efficient purification can result in serious side effects due to the cellular impurities [7,8]. Therefore, there is a great demand for high-efficiency FMDV purification techniques which could be used during the vaccine manufacturing process.

First and foremost, any purification technique for FMDV should ensure the integrity of 146S particles throughout the purification process. At present, the major reported purification methods for inactivated FMDV vaccines include sucrose density gradient centrifugation (SDG) [9], polyethylene glycol precipitation [5,10], sodium sulfate precipitation [11], ultrafiltration [5,12], aqueous two-phase partition [11] and chromatography [13,14]. However, there are difficulties in terms of the technical promotion and purification efficiency of these methods.

To overcome these difficulties, we developed a new affinity purification method for inactivated FMDV vaccines using Gram-positive enhancer matrix (GEM) particles coupled to a peptidoglycan-binding protein anchor (PA) [15–18] and a

\* Corresponding authors at: Institute of Veterinary Immunology & Engineering, Jiangsu Academy of Agricultural Sciences, Nanjing 210014, China.

E-mail addresses: [qxwshyi2011@hotmail.com](mailto:qxwshyi2011@hotmail.com) (X. Qiao), [immun\\_tech@163.com](mailto:immun_tech@163.com) (Q. Zheng).

<sup>1</sup> Contributed equally to this article.

FMDV-specific nanobody (Nb) [19–23]. The GEM particles were prepared from acid-pretreated food-grade *Lactococcus lactis* bacteria [15], which retained the intact peptidoglycan envelope without cellular components or recombinant DNA [16]. The PA, which was derived from the *L. lactis* AcmA cell-wall hydrolase, could be non-covalently attached to the surface of GEM particles through peptidoglycans with high affinity [17]. The strong binding of recombinant proteins or peptides containing a PA domain to GEM particles could provide an efficient and simple purification method [15].

Nanobodies, which were first discovered in the sera of *camelidae* (such as llamas, dromedaries and camels), are unique antibodies for lack of variable light chain (VL) [19]. As the smallest known functional antibody fragments, Nbs are only 15 kDa in size and their affinities are similar to those of conventional antibodies [20–22]. However, compared with conventional antibodies, Nbs exhibit many advantages such as solubility, stability and their single-domain structure [22,23], which enables the application of Nbs in immunoassays, the tracing of antigens in living cells and as capture molecules for the precipitation of protein complexes [24–28].

The feasibility and applicability of the GEM particle-PA system to display and purify heterologous proteins has been investigated in our laboratory. In previous reports, porcine circovirus (PCV) 2 Cap protein [18], cholera toxin subunit A1 [29] and porcine reproductive and respiratory syndrome virus (PRRSV) [30] have been successfully displayed and purified.

Here, we hypothesized that a Nb against 146S particles could be selected and displayed to the surface of GEM particles through fusion to PA, and the developed GEM-PA-nanotrap would have the potential for purification of the corresponding FMDV strain. FMDV serotype O is the most globally prevalent of the seven different serotypes and has led to enormous economic losses [31,32], therefore, FMDV vaccine strain O/MYA98/BY/2010 was selected as a model analyte. In this study, we focused on characterization of the GEM-PA-nanotrap and its performance in the purification of FMDV.

## 2. Materials and methods

### 2.1. Materials

Inactivated FMDV serotype A, O and Asia I antigens and serotype-specific rabbit antisera were provided by China Agricultural Vet. Bio. Science and Technology Co., Ltd. *L. lactis* MG1363 was purchased from the China Committee for Culture Collection of Microorganisms (Beijing, China). Horseradish peroxidase (HRP)-labeled goat anti-rabbit IgG (H+L), HRP-labeled goat anti-mouse IgG (H+L) and tetramethylbenzidine (TMB) were from Sigma-Aldrich (St. Louis, MO, USA). Mouse anti-HA tag antibody was from Covance (Princeton, NJ, USA). Trizol was from Invitrogen (USA). ReverTra Ace- $\alpha$ - was from Toyobo (Japan). The HisTrap HP metal affinity chromatography column was from GE Healthcare (USA). Restriction enzymes *Pst* I, *Not* I, *Nde* I, *Xho* I and T4 DNA ligase were from NEB (USA). The phagemid vector pMECS, M13K07 helper phages, and *Escherichia coli* TG1 and WK6 cells were provided by Prof. Yakun Wan's laboratory (CAS Key Laboratory of Receptor Research, Shanghai Institute of Materia Medica, Chinese Academy of Sciences, Shanghai, China). Ultracentrifugation was performed using the Optima L-100 XP ultracentrifuge (Beckman Coulter, CA, USA). Affinity analysis was performed using the Biacore™ X100 Plus instrument (GE Healthcare, UK). Chromatography analysis was performed using an Agilent 1260 HPLC series system (Agilent, USA). All other reagents were of analytical grade.

### 2.2. Nanobody generation and characterization

Nanobodies against 146S particles were prepared and characterized as described previously with modifications [33]. The details are provided as [supplementary material](#).

Bactrian camel and pigs used as experimental animals were treated in strict accordance with the recommendations in the guide for the regulation for the Administration of Affairs concerning Experimental Animal of the People's Republic of China. Animal experiments were approved by Jiangsu Academy of Agricultural Sciences Experimental Animal Ethics Committee (Permit Number: NKYVET 2015-0066). All efforts were made to minimize their suffering.

### 2.3. Construction and expression of the PA-Nb fusion protein

The plasmid encoding PA was stored in our laboratory, and the PA-Nb fusion protein was cloned and expressed as described previously with some modifications [18]. The pET-32a-PA-Nb expression vector was constructed by the insertion of genes encoding PA and Nb into the *Nde* I-*Xho* I double-digested pET-32a vector. The pET-32a-PA-Nb expression vector was confirmed by double-digestion and transformed into *E. coli* BL21. An unrelated Nb was used to construct the negative control and *E. coli* BL21 (DE3) cells transformed with the pET-32a vector were used as a blank control.

Transformants were grown in Luria-Bertani (LB) medium containing 100  $\mu$ g/mL of ampicillin to express the PA-Nb fusion protein upon induction with 1 mM isopropyl  $\beta$ -D-1-thiogalactopyranoside (IPTG) at 16 °C overnight. After a centrifugation step (10 min, 8000g at 4 °C), the cells were harvested and resuspended in phosphate-buffered saline (PBS), pH 7.2. The PA-Nb fusion protein was prepared by sonication, and after a centrifugation step (10 min, 17,000g at 4 °C) the soluble fraction and the precipitate were analyzed by sodium dodecyl sulfate polyacrylamide gel electrophoresis (SDS-PAGE) and western blotting. Briefly, the PA-Nb fusion protein and pre-stained SDS-PAGE standards (Fermentas, USA) were electrophoresed on a 12% polyacrylamide gel and transferred onto nitrocellulose membrane using a semidry electroblotter (Bio-Rad, USA). After blocking with 5% (w/v) skimmed milk for 1 h at 37 °C, the mouse anti-His antibody and HRP-labeled goat anti-mouse IgG (H+L) were added and incubated for 1 h at 37 °C, respectively. Diaminobenzidine (DAB, Sigma) was used as the peroxidase substrate.

Endotoxin of the PA-Nb-containing soluble fraction was removed by Triton X-114 [34]. Briefly, Triton X-114, at a final concentration of 0.6%, was added into the PA-Nb-containing soluble fraction and the mixture was incubated at 37 °C for 2 h. After a centrifugation step (10 min, 12,000g at 4 °C), the supernatant was treated with Triton X-114 for twice. After an endotoxin removal procedure, the Triton X-114 residues were efficiently removed by ultrafiltration. The endotoxin content of the PA-Nb-containing soluble fraction was determined using the compendial *limulus* amoebocyte lysate (LAL) assay (Lonza, USA) [35,36] according to the manufacturer's protocol.

### 2.4. Construction of GEM-PA-nanotrap

GEM particles were prepared as described previously [16,18]. Briefly, GEM particles were obtained by boiling freshly grown *L. lactis* MG1363 cells in 0.1 M HCl (pH 1) for 30 min, followed by extensive washing with PBS. One unit (U) was defined as  $2.5 \times 10^9$  GEM particles. GEM particles were added into the PA-Nb-containing soluble fraction and incubated for 30 min on an end-over-end rotor at room temperature. The PA-Nb fusion protein rapidly bound to the GEM particles, which were both present in solution. After a centrifugation step (5 min, 6000g at 4 °C), the resulting GEM-PA-Nb complexes (referred to as GEM-PA-

nanotrap) were analyzed by SDS-PAGE and western blotting. The GEM-PA-nanotrap was collected and stored in PBS at a concentration of 1 U/mL at  $-80^{\circ}\text{C}$  until use.

### 2.5. Immunoprecipitation of FMDV

The GEM-PA-nanotrap (1 U) was mixed with 10 mL of inactivated FMDV suspension (the input fraction) and 10 mL of BHK-21 cell suspension, each pretreated by sonication. After incubation at  $37^{\circ}\text{C}$  for 1 h on an end-over-end rotor and a centrifugation step (10 min, 12,000g at  $4^{\circ}\text{C}$ ), the supernatant (the non-bound fraction) and precipitate (the bound fraction) were analyzed by SDS-PAGE, western blotting and high-performance size exclusion chromatography (HPSEC) to determine the FMDV recovery and purification efficiency. HPSEC analysis was performed as described previously with some modifications [37,38]. The Agilent 1260 HPLC series system (Agilent, USA) was equipped with a degasser and a variable wavelength detector with UV monitoring at 280 nm and 259 nm. For each assay, 100  $\mu\text{L}$  of sample was injected and eluted at 0.6 mL/min in a mobile phase of 50 mM phosphate buffer (pH 7.2) containing 100 mM  $\text{Na}_2\text{SO}_4$ .

In accordance with Announcement No. 2078 of the Ministry of Agriculture and Rural Affairs of the People's Republic of China, the total protein concentration of inactivated FMDV vaccines must be below 500  $\mu\text{g}/\text{mL}$  and the maximum endotoxin content must be below 50 endotoxin units (EUs) per dose [39]. Therefore, the total protein concentration and the endotoxin content of the input, non-bound and bound fractions were determined using the Pierce BCA protein assay kit (Thermo Fisher Scientific) and compendial *limulus* amebocyte lysate (LAL) assay (Lonza, USA) [35,36], respectively, according to the manufacturers' protocols.

### 2.6. Immunogenicity of purified FMDV

To determine whether the purification process would affect the structural integrity and immunogenicity of 146S particles, both unpurified and purified FMDV were used for immunization. The virions were mixed with 206 adjuvant (Seepic, France), while PBS was used as a negative control. As 10 mL of inactivated FMDV suspension was used for purification and the concentration of 146S particles was 5  $\mu\text{g}/\text{mL}$ , the purified FMDV was adjusted with PBS to its original volume of 10 mL.

Healthy landrace pigs ( $n = 30$ ), aged 6–7 weeks, were selected from a FMDV-free farm. All animals were tested using routine serological assays and confirmed to be free of FMDV, PRRSV and PCV prior to immunization. The pigs were randomly divided into three groups (each group consisting of 10 pigs) and the immunization strategies were shown in Table 1. Serum samples were collected from all pigs at 28 days post-immunization (dpi) and serum antibody titers against FMDV were evaluated according to the liquid-phase blocking enzyme-linked immunosorbent assay (LPB-ELISA) kit.

## 3. Results

### 3.1. Preparation of 146S particles

Crude FMDV antigens contained many cellular proteins, as shown by SDS-PAGE (Fig. S1), most of which were from the BHK-

21 cells. 146S particles were purified by SDG and analyzed by SDS-PAGE and western blotting (Figs. S1 and S2). The molecular weights of the structural proteins VP1, VP2 and VP3 were between 25 and 35 kDa [40], and the purified 146S particles contained three bands migrating in this range (Figs. S1 and S2), which presumably represented these proteins. The  $\text{OD}_{259\text{ nm}}$  of the purified 146S particles was determined and the final concentration of these purified particles was 20.0  $\mu\text{g}/\text{mL}$  [32].

### 3.2. Serological assays

A non-immunized Nb library was constructed after serological assays of a healthy bactrian camel by LPB-ELISA. The LPB-ELISA results indicated that the camel was an appropriate source for construction of the non-immunized Nb library, which had no detectable FMDV-specific antibody titer even at a dilution of 1:2 (Table S1).

### 3.3. Construction of the non-immunized Nb library

To construct the non-immunized Nb library (Fig. S3), peripheral blood lymphocytes were taken from the non-immunized camel and total RNA was extracted to prepare a cDNA library. Nb genes were amplified and ligated into the pMECS phagemid vector, followed by transformation into *E. coli* TG1 cells. The resulting transformants were used to construct the non-immunized Nb library and Nbs were fused for expression with the phage minor coat protein on the surface of filamentous phage after rescued with M13K07 helper phage.

The capacity of the non-immunized Nb library was estimated to be  $10^{11}$  and almost all of the transformants contained a single Nb gene insertion fragment determined by colony PCR (Fig. S4). Thirty-three randomly selected transformants were sequenced to evaluate the integrity and diversity of the non-immunized library. The framework regions (FRs) and complementary determining regions (CDRs) were determined according to Kabat numbering [41] (Fig. S5) and all of the sequences were found to be the correct reading frame. The length of CDR1 ranged from about 9–10 amino acid residues, with an average length of 10 residues, CDR2 ranged from about 5–11 amino acid residues, with an average length of 7 residues and CDR3 ranged from about 8–23 amino acid residues, with an average length of 19 residues. Four conserved hallmark residues in FR2 (Phe37, Glu44, Arg45 and Gly47) and a second intra-domain disulfide bond connecting CDR1 and CDR3 were present, which were coincident with previous reports [42]. This indicated that all of the clones were derived from the heavy-chain antibody specific germline genes and a high-quality non-immunized Nb library had been successfully constructed.

### 3.4. Bio-panning

After being displayed on the surface of filamentous phage upon super-infection with M13K07 helper phage, Nbs were used for affinity screening against 146S particles. Three consecutive rounds of affinity screening were performed and approximately  $10^{11}$  phage particles were used for each round. Any Nbs with reactivity against BHK-21 antigens or 12S particles were removed by pre-incubation with these antigens before affinity screening against 146S particles. To improve the affinity and specificity of the

**Table 1**  
Experimental groups and immunization strategies.

No. of group	Antigen	Adjuvant	Immunization route	Number of pigs	Immunizing dose (mL/pig)
1	Unpurified FMDV	206	Intramuscular	10	2
2	Purified FMDV	206	Intramuscular	10	2
3	PBS	206	Intramuscular	10	2

**Table 2**  
Process monitoring of the bio-panning.

Round	Antigen concentration ( $\mu\text{g}/\text{mL}$ )	Titer of input phage	Titer of output phage	Enriching factor <sup>1</sup>
1st	10	$1.51 \times 10^{11}$	$1.25 \times 10^5$	$0.83 \times 10^{-6}$
1st-C <sup>2</sup>	– <sup>3</sup>	$1.26 \times 10^{11}$	$1.46 \times 10^5$	$1.16 \times 10^{-6}$
2nd	8	$1.74 \times 10^{11}$	$5.27 \times 10^6$	$3.03 \times 10^{-5}$
2nd-C	–	$1.58 \times 10^{11}$	$1.38 \times 10^5$	$0.87 \times 10^{-6}$
3rd	4	$1.49 \times 10^{11}$	$3.85 \times 10^7$	$2.58 \times 10^{-4}$
3rd-C	–	$1.62 \times 10^{11}$	$1.06 \times 10^5$	$0.65 \times 10^{-6}$

<sup>1</sup> Enriching factor was calculated by computational formula (output/input).

<sup>2</sup> The control well of the first round of panning.

<sup>3</sup> No antigen coating.

selected Nbs, the concentration of 146S particles was reduced over the three rounds (10, 8 and 4  $\mu\text{g}/\text{mL}$  for rounds 1, 2 and 3, respectively) and the frequency, stringency and time of washing were also increased. The enrichment factor increased stably over the three consecutive rounds of affinity screening and the output phage particles after the third round increased more than 100-fold compared with the first round (Table 2). These data demonstrated strong enrichment of 146S particle-specific phage particles, while no enrichment was observed in the control wells (Fig. S6).

### 3.5. Selection of 146S particle-specific Nbs

In total, 480 individual clones were picked randomly to identify the 146S particle-specific Nbs by periplasmic extract ELISA (PE-ELISA) after the affinity screening. A total of 105 clones showed binding activity against FMDV, whereas no reactivity against BHK-21 antigens (Figs. S7–S18). Upon sequence analysis, the 105 clones were classified into 41 unique FMDV-specific Nbs (Fig. S19). To identify 146S particle-specific Nbs, all of the 41 Nbs was tested against 146S particles, 12S particles, trypsin-treated virions and the denatured virions.

Of the 41 Nbs, 33 reacted with both the 146S particles and 12S particles, whereas no reactivity was detected against either trypsin-treated virions or denatured virions (Figs. S20–S22). As both 146S particles and 12S particles shared the same epitopes of the GH-loop, which could be destroyed by trypsin [43,44], the PE-ELISA results suggested that these 33 Nbs were specific to the FMDV GH-loop. Furthermore, six Nbs reacted with 146S particles, 12S particles and the trypsin-treated virions, whereas no reactivity was detected against the denatured virions (Fig. S23), indicating the specificity for 12S particles and non-reactivity with the GH-loop. Only two Nbs reacted with both 146S particles and the trypsin-treated virions, whereas no reactivity was detected with either 12S particles or the denatured virions (Fig. S24), indicating that these Nbs had specificity for the 146S particle-specific epitopes. None of the Nbs could react with the denatured virions, suggesting that all of the 41 Nbs were specific for conformational epitopes that only presented on native FMDV virions.

In summary, two 146S particle-specific Nbs were identified by PE-ELISA. All of the sequences contained the hallmark amino acid residues in FR2 and CDR3 (Fig. S25). Although the amino acid sequences showed great differences in the CDR regions, suggesting that the Nbs would react with different epitopes [45], they still showed 63.8% sequence homology with each other. As other proteins expressed along with the periplasmic proteins could affect the PE-ELISA, the absorbance values of 146S particles may be higher, while those of the control and BHK-21 antigens may be lower after purification.

### 3.6. Expression and purification of Nbs

The 146S particle-specific Nb45 and Nb205 were expressed in *E. coli* WK6 cells [46] and purified by Ni-NTA affinity chromato-

graphy. Following identification by SDS-PAGE and western blotting, Nbs with a molecular weight of about 17 kDa (Fig. 1) were successfully expressed and purified.

### 3.7. Specificity assays

The specificity of Nb45 and Nb205 was determined by double antibody sandwich ELISA (DAS-ELISA) with FMDV serotypes O, A and Asia 1. Both Nbs showed high specificity to FMDV serotype O and no cross-reactivity with serotypes A and Asia 1 (Fig. 2). It could be concluded that both Nb45 and Nb205 were specific to FMDV serotype O.

### 3.8. Binding affinity

Kinetic analysis with Biacore was performed to evaluate the affinities of Nb45 and Nb205. A blank injection was included and the Nbs with a concentration of 4.575 nM were tested in duplicate. As the sensorgrams (Fig. S26) showed, the equilibrium dissociation constant ( $K_D$ ) values of Nb45 and Nb205 were  $4.02 \times 10^{-10}$  M and  $8.38 \times 10^{-11}$  M, respectively (Table 3), which were higher than other Nbs selected previously [33,47–51]. These results showed that Nb45 and Nb205 had high affinity with 146S particles.

### 3.9. Expression of the PA-Nb fusion protein

Nb205 was used in subsequent experiments because of its favorable  $K_D$  value. The PA and Nb205 fragments were amplified and the PA-Nb205 fragment was assembled by splicing overlap extension PCR (SOE-PCR) (Fig. S27). The pET-32a-PA-Nb expression vector was constructed and confirmed by double-digestion (Fig. S27).

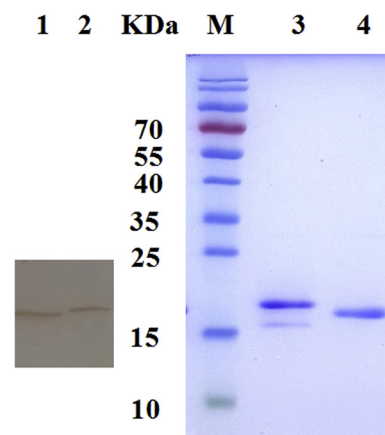


**Fig. 1.** SDS-PAGE analysis and western blot assay of two 146S particle-specific nanobodies (of about 17 kDa). Lanes 1 and 2: Western blot assay of Nb45 and Nb205; Lanes 3 and 4: SDS-PAGE analysis of Nb205 and Nb45; Lane M: protein standards.

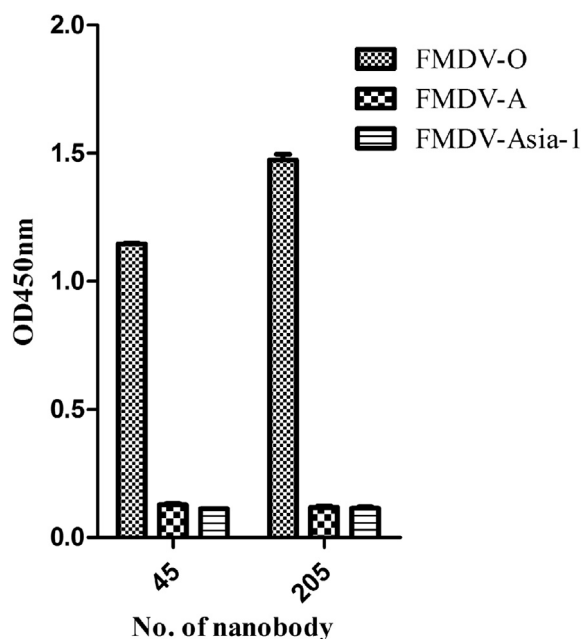


**Fig. 2.** DAS-ELISA analysis of the cross-reactivity of Nb45 and Nb205 with other FMDV serotypes (in triplicate). FMDV serotypes O, A and Asia 1 were used for the assessment of specificity. The error bars represent the standard deviation.

The PA-Nb205 fusion protein was expressed in *E. coli* BL21 (DE3) cells, and the periplasmic extracts and precipitates were collected after sonication and centrifugation. SDS-PAGE analysis revealed the presence of PA-Nb205 fusion protein in both the periplasmic extracts and precipitates, with a molecular weight of about 38 kDa (Fig. S28). Western blot analysis indicated the specific reactivity of PA-Nb205 fusion protein with the mouse anti-His tag antibody (Fig. S28).

After sonication and centrifugation, the endotoxin content of the PA-Nb-containing soluble fraction was above 60,000 EU/mL, as determined using the LAL assay (Lonza, USA). The endotoxin of the PA-Nb-containing soluble fraction was removed by treatment with Triton X-114 for three times, until the content was below 5 EU/mL.

### 3.10. Construction of GEM-PA-nanotrap

To construct the GEM-PA-nanotrap (Fig. 3), GEM particles were added into PA-Nb205-containing periplasmic extracts. After incubation and a centrifugation step (5 min, 6000g at 4 °C), the GEM-PA-Nb205 complexes were separated and analyzed by SDS-PAGE and western blotting. SDS-PAGE analysis revealed that the PA-Nb205 fusion protein was only present in the precipitate, with a molecular weight of about 38 kDa (Fig. 4). Western blot analysis confirmed this result and no PA-Nb205 fusion protein was found in the supernatant (Fig. 4). In summary, the PA-Nb205 fusion protein was separated from the periplasmic extracts and displayed on

the surface of GEM particles. By comparative protein gel electrophoresis experiments using bovine serum albumin as a standard, we estimated that 1 U of GEM particles could bind to 50  $\mu$ g of the PA-Nb205 fusion protein. The endotoxin content of the GEM-PA-Nb205 complexes was below 5 EU/mL.

### 3.11. Purification of FMDV

After incubation and centrifugation, the supernatant (non-bound fraction) and precipitate (bound fraction) were analyzed to evaluate the purification effect by SDS-PAGE followed by immunoblotting with anti-FMDV antibody. SDS-PAGE and western blot analysis revealed that both the non-bound and bound fractions contained bands between 25 and 35 kDa, which represented FMDV structural proteins (Fig. 5A). The PA-Nb205 fusion protein was only found in the bound fraction with a molecular weight of about 38 kDa (Fig. 5A). The bound fraction was washed for three times with PBST and FMDV virions were dissociated from the GEM-PA-nanotrap using 1% SDS after the last wash. After centrifugation (5 min, 6000g at 4 °C), FMDV virions were collected in the supernatant with three bands between 25 and 35 kDa, corresponding to the FMDV structural proteins VP1, VP2 and VP3 (Fig. 5B).

The feasibility of detecting FMDV particles using HPSEC has been investigated, 146S particles and 12S particles show characteristic peaks at about 13 min and 16 min, respectively [37,38]. Here, the input, non-bound and bound fractions were analyzed by HPSEC to evaluate the purification effect. In the input fraction, the peak around 12.4 min was identified as 146S particles and the peak around 16.6 min was identified as 12S particles (Fig. 6A). After purification by the GEM-PA-nanotrap, only one specific peak around 12.4 min was detected in the bound fraction, which was thought to represent purified 146S particles (Fig. 6B). The absence of a peak around 12.4 min indicated that no 146S particles were remaining, while a peak at around 16.7 min indicated that 12S particles still remained in the non-bound fraction (Fig. 6C). The results indicated that almost all of the 146S particles were purified by the GEM-PA-nanotrap and total FMDV recovery was more than 99%.

The total protein concentrations of the input, non-bound and bound fractions were determined to be 3.0, 2.9 and 0.05 mg/mL, respectively, using the Pierce BCA protein assay kit (Thermo Fisher Scientific). FMDV recovery from the GEM-PA-nanotrap was defined as the ratio of bound fraction to the initial input fraction, which was about 1.7%, while the efficiency of nonviral protein removal was about 98.3%. The total protein concentration in the bound fraction conformed with the standard set by the Ministry of Agriculture and Rural Affairs of the People's Republic of China (below 500  $\mu$ g/mL), and the endotoxin content was below 5 EU/mL, which also met the standard (below 50 EU/mL).

### 3.12. Serum antibody assays

The serum antibody titers of the unpurified and purified FMDV immunized groups at 28 dpi were measured using the LPB-ELISA kit. The results of LPB-ELISA showed that the FMDV-specific antibody titers of the unpurified and purified FMDV immunized groups

**Table 3**  
Sensorgrams and kinetic parameters of binding between the nanobody and 146S particles.

No. of nanobody	<sup>1</sup> $k_a$ ( $M^{-1} s^{-1}$ )	<sup>2</sup> $k_d$ ( $s^{-1}$ )	<sup>3</sup> $K_D$ (M)	$R_{max}$ (RU)
45	$2.236 \times 10^6$	$8.987 \times 10^{-4}$	$4.02 \times 10^{-10}$	111.9
205	$1.074 \times 10^6$	$9.002 \times 10^{-5}$	$8.38 \times 10^{-11}$	361.5

<sup>1</sup>  $k_a$  association rate constant.

<sup>2</sup>  $k_d$  dissociation rate constant.

<sup>3</sup>  $K_D$  the equilibrium dissociation constant.

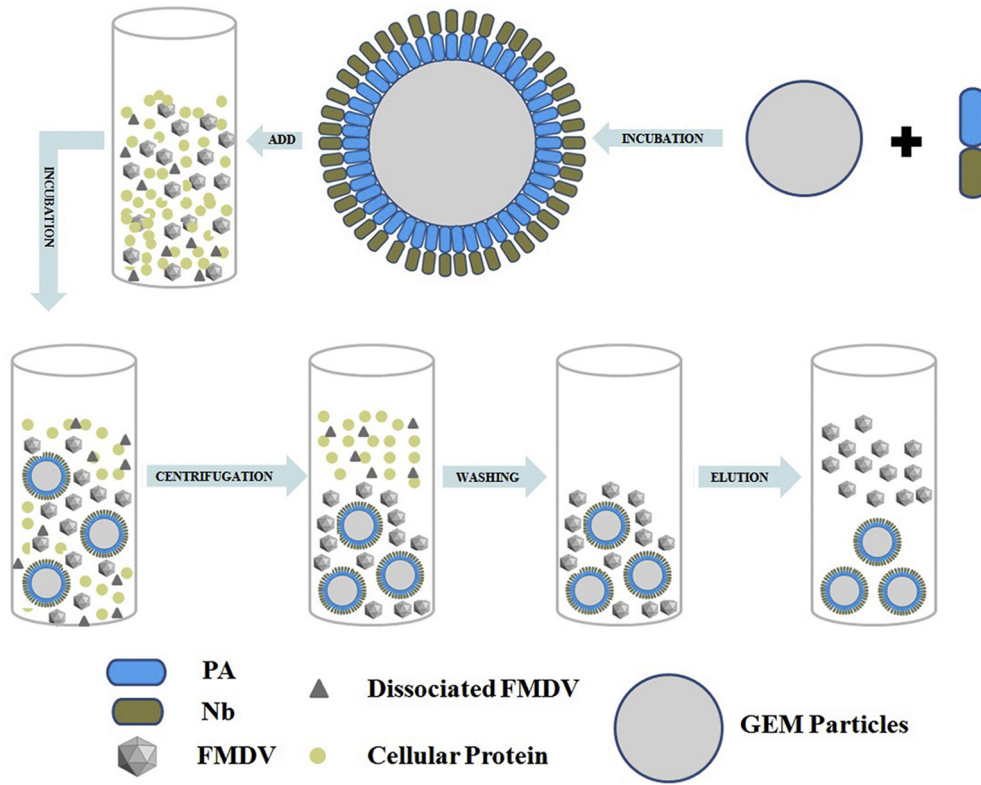


Fig. 3. Schematic representation of the GEM-PA-nanotrap generation and purification strategy.

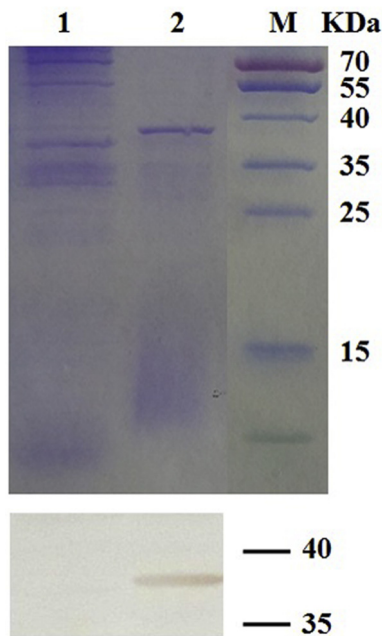


Fig. 4. SDS-PAGE analysis (top) and western blot assay (bottom) of the GEM-PA-Nb complexes. Lane 1: SDS-PAGE analysis of the supernatant after incubation with GEM particles and centrifugation; Lane 2: SDS-PAGE analysis of the precipitate after incubation with GEM particles and centrifugation; Lane M: protein standards.

were similar, with no significant differences ( $P > 0.05$ ) (Fig. 7). As expected, the sera from pigs immunized with PBS displayed no LPB antibody activity. Pigs immunized with purified FMDV showed no side effects or other clinical manifestations over the observation period.

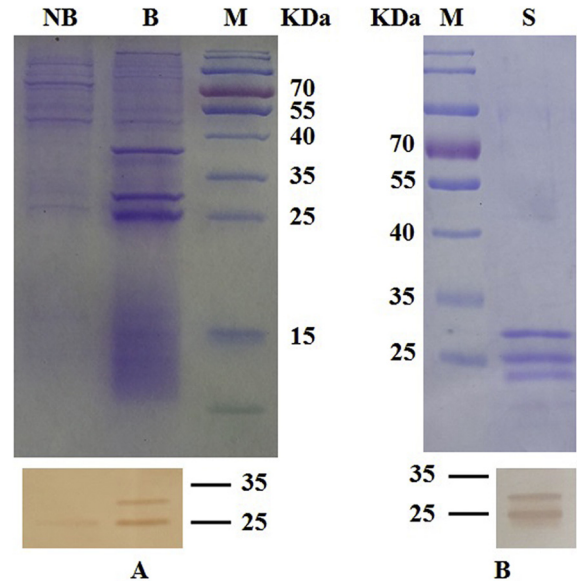
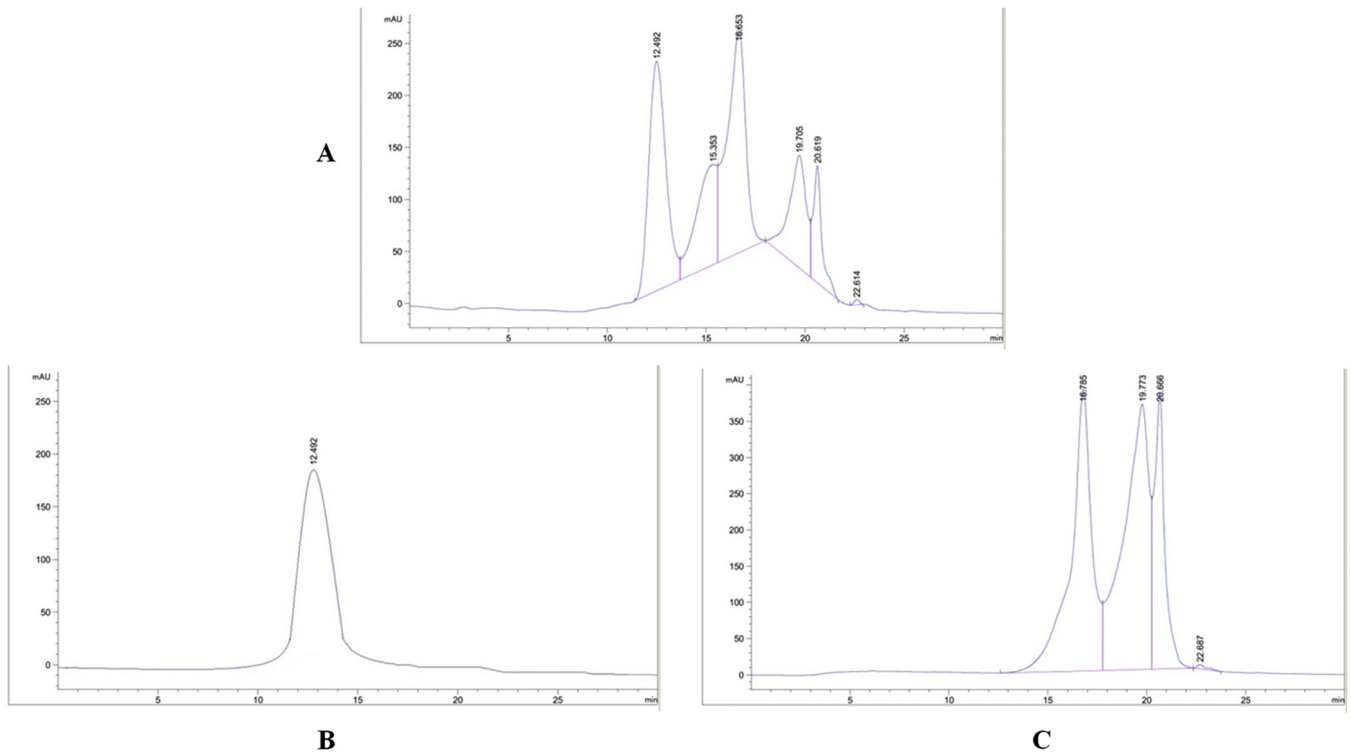


Fig. 5. Purification of FMDV using the GEM-PA-nanotrap. A: For purification of FMDV, soluble fractions of cellular lysates were incubated with the GEM-PA-nanotrap. After centrifugation, the non-bound (NB) and bound fractions (B) were analyzed by SDS-PAGE and visualized either by Coomassie Blue (top) or by immunoblot analysis (bottom). B: To collect FMDV, the bound fraction was washed for three times with PBST and dissociated by 1% SDS. After centrifugation, the supernatant (S) was collected and analyzed by SDS-PAGE and visualized either by Coomassie Blue (top) or by immunoblot analysis (bottom).

#### 4. Discussion

In this study, an effective affinity purification method called GEM-PA-nanotrap was developed and used for the purification of 146S particles of the FMDV vaccine strain O/MYA98/BY/2010.



**Fig. 6.** HPSEC analysis of FMDV during the purification process. A: HPSEC analysis of FMDV in the input fraction; B: HPSEC analysis of FMDV in the bound fraction; C: HPSEC analysis of FMDV in the non-bound fraction.

The GEM-PA-nanotrap was constructed based on the GEM particle-PA system and a FMDV-specific Nb. As the smallest known functional antibody fragments, the CDR3 fragments of Nbs form convex structures and possess a superior ability to bind some cryptic epitopes that could not be accessed by conventional antibodies [22,23]. These characteristics may make Nbs the ideal candidates to differentiate 146S particles from 12S particles. To select 146S particle-specific Nbs, a high-quality non-immunized Nb library was constructed. A 12S particle-depletion step was performed during affinity screening and two 146S particle-specific Nbs were selected (Nb45 and Nb205). ELISA results revealed that these two Nbs were specific to 146S particles of FMDV serotype O without cross-reactivity with FMDV serotypes A and Asia 1. The  $K_D$  values of Nb45 and Nb205 were  $4.02 \times 10^{-10}$  M and  $8.38 \times 10^{-11}$  M, respectively, which represented higher affinities than previously selected Nbs [33,47–51].

The PA-Nb fusion protein, which was expressed in the prokaryotic expression system with a molecular weight of about 38 kDa (Fig. 4), could rapidly bind GEM particles after incubation. With the constructed GEM-PA-nanotrap, about 50  $\mu$ g of the PA-Nb fusion protein was displayed on the surface of GEM particles, which was not the maximum binding quantity described in previous reports [17]. Therefore, the concentration of IPTG and the expression conditions need to be optimized to increase the expression level of the PA-Nb fusion protein. As the presence of lipopolysaccharide in the Gram-negative cell wall has been suggested as a potential problem for vaccine applications, the endotoxin content of the GEM-PA-nanotrap was checked and was found to be below 5 EU/mL, as verified by LAL assays.

The GEM-PA-nanotrap (1 U) was used to purify about 10 mL of inactivated FMDV suspension, but this was not thought to be the maximum purification quantity for the GEM-PA-nanotrap. After incubation and centrifugation, the 146S particles were pulled down in the bound fraction and the purification efficiency was

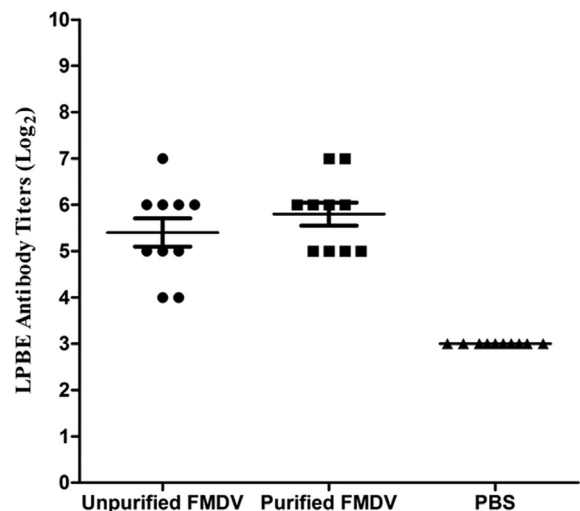


**Fig. 7.** Antibody responses in pigs induced by unpurified FMDV, purified FMDV and PBS. Serum samples were collected at 28 dpi to determine the FMDV-specific LPB antibody titers. Antibody titers were expressed as the reciprocal  $\log_2$  of the serum dilutions.

evaluated by HPSEC and SDS-PAGE, followed by immunoblotting. SDS-PAGE and western blot analysis revealed that the 146S particles were collected with three bands between 25 and 35 kDa, corresponding to the structural proteins VP1, VP2 and VP3 (Fig. 5B). 146S particles were purified without any other dissociated subunits, as only one specific peak at about 12.4 min was detected and no other peaks were observed in the bound fraction by HPSEC (Fig. 6B). The peak at about 12.4 min disappeared and other peaks were still detected in the non-bound fraction, which indicated that none of the 146S particles were detected but significant amounts

of the dissociated subunits remained in the non-bound fraction, which could not be purified by the GEM-PA-nanotrap (Fig. 6C). These results clearly indicated that almost all of the 146S particles were purified by the GEM-PA-nanotrap and the total FMDV recovery was more than 99%. The total protein concentration of the bound fractions was only 0.05 mg/mL, while the protein concentration of the input fraction of inactivated FMDV suspension was about 3 mg/mL and the efficiency of nonviral protein removal was about 98.3%. The endotoxin content of the bound fraction was below 5 EU/mL. Both 146S particles and other dissociated subunits were present in the input fraction of inactivated FMDV suspension before purification, as identified by HPSEC (Fig. 6A), suggesting that a small fraction of 146S particles has been dissociated during storage.

The purified 146S particles were used for immunization to determine whether the purification process would affect the integrity and immunogenicity of 146S particles. The LPB-ELISA antibody titers of pigs immunized with unpurified and purified FMDV were similar and showed no significant differences between groups ( $P$  greater than 0.05) (Fig. 7), which indicated that the purification process had no effect on the integrity and immunogenicity of 146S particles. No side effects or clinical manifestations were observed in pigs immunized with the purified FMDV throughout the experiment.

In summary, all of these data confirmed that structurally intact 146S particles with high purity were purified by the GEM-PA-nanotrap. The GEM-PA-nanotrap has the potential to be an efficient and operable method for the recovery and purification of FMDV from cell lysate. Our work also confirmed the effectiveness of the non-immunized Nb library constructed in this study. In future work, the GEM-PA-nanotrap method will be optimized for purification of FMDV during the vaccine manufacturing process.

## Acknowledgements

This work was supported by the National Natural Science Foundation (31802220). We wish to thank Dr. YK Wan (Chinese Academy of Sciences, Shanghai) for providing the vector, helper phage and *Escherichia coli* strains. We thank Liwen Bianji, Edanz Editing China ([www.liwenbianji.cn/ac](http://www.liwenbianji.cn/ac)), for editing the English text of a draft of this manuscript.

## Conflicts of interest

The authors have no financial conflicts of interest.

## Contributions

JH, XQ, QZ conceived the study. HC, JC, ZC, LD designed the study. HC, JC acquired the data. All authors analyzed and interpreted the data. HC, JC, ZC, LD drafted the article and all authors provided critical revisions to the content. All authors had full access to the data, took part in meetings to discuss and interpret the results, drafted or critically revised the report, and approved its final version.

## Appendix A. Supplementary material

Supplementary data to this article can be found online at <https://doi.org/10.1016/j.vaccine.2019.04.078>.

## References

- Cartwright B, Chapman WG, Brown F. Serological and immunological relations between the 146S and 12S particles of foot-and-mouth disease virus. *J Gen Virol* 1980;50:369–75.
- Doel TR, Chong WK. Comparative immunogenicity of 146S, 75S and 12S particles of foot-and-mouth disease virus. *Arch Virol* 1982;73:185–91.
- Brown F, Cartwright B. Dissociation of foot-and-mouth disease virus into its nucleic acid and protein components. *Nature* 1961;192:1163–4.
- Liang T, Yang D, Liu M, Sun C, Wang F, Wang J, et al. Selection and characterization of an acid-resistant mutant of serotype O foot-and-mouth disease virus. *Arch Virol* 2014;159:657–67.
- Pay TWF, Hingley PJ. Correlation of 140S antigen dose with the serum neutralizing antibody-response and the level of protection induced in cattle by foot-and-mouth-disease vaccines. *Vaccine* 1987;5:60–4.
- Rao MG, Butchiah G, Sen AK. Antibody-response to 146S particle, 12S protein subunit and isolated VP1 polypeptide of foot-and-mouth-disease virus type asia-1. *Vet Microbiol* 1994;39:135–43.
- Doel TR. FMD vaccines. *Virus Res* 2003;91:81–99.
- Rodriguez LL, Grubman MJ. Foot and mouth disease virus vaccines. *Vaccine* 2009;27:90–4.
- Barteling SJ, Meloen RH. A simple method for the quantification of 140S particles of foot-and-mouth disease virus (FMDV). *Arch Virol* 1974;45:362–4.
- Feng X, Ma JW, Sun SQ, Guo HC, Yang YM, Jin Y, et al. Quantitative detection of the foot-and-mouth disease virus serotype O 146S antigen for vaccine production using a double-antibody sandwich ELISA and nonlinear standard curves. *PLoS One* 2016;11(3):e0149569.
- Vanmaanen C, Terpstra C. Quantification of intact 146S foot-and-mouth-disease antigen for vaccine production by a double antibody sandwich elisa using monoclonal-antibodies. *Biologicals* 1990;18:315–9.
- Yang M, Holland H, Clavijo A. Production of monoclonal antibodies against whole virus particles of foot-and-mouth disease virus serotype O and A and their potential use in quantification of intact virus for vaccine manufacture. *Vaccine* 2008;26:3377–82.
- Du P, Sun S, Dong J, Zhi X, Chang Y, Teng Z, et al. Purification of foot-and-mouth disease virus by heparin as ligand for certain strains. *J Chromatogr B* 2017;1049:16–23.
- Liang S, Yang Y, Sun L, Zhao Q, Ma G, Zhang S, et al. Denaturation of inactivated FMDV in ion exchange chromatography: evidence by differential scanning calorimetry analysis. *Biochem Eng J* 2017;124:99–107.
- Audouy SAL, van Roosmalen ML, Neef J, Kanninga R, Post E, Deemter M, et al. Lactococcuslactis GEM particles displaying pneumococcal antigens induce local and systemic immune responses following intranasal immunization. *Vaccine* 2006;24:5434–41.
- Van Roosmalen ML, Kanninga R, El Khattabi M, Neef J, Audouy S, Bosma T, et al. Mucosal vaccine delivery of antigens tightly bound to an adjuvant particle made from food-grade bacteria. *Methods* 2006;38:144–9.
- Bosma T, Kanninga R, Neef J, Audouy SAL, van Roosmalen ML, Steen A, et al. Novel surface display system for proteins on non-genetically modified gram-positive bacteria. *Appl Environ Microb* 2006;72:880–9.
- Li PC, Qiao XW, Zheng QS, Hou JB. Immunogenicity and immunoprotection of porcine circovirus type 2 (PCV2) Cap protein displayed by *Lactococcuslactis*. *Vaccine* 2016;34:696–702.
- Hamers-Casterman C, Atarhouch T, Muyldermans S, Robinson G, Hamers C, Songa EB, et al. Naturally occurring antibodies devoid of light-chains. *Nature* 1993;363:446–8.
- Desmyter A, Transue TR, Ghahroudi MA, Thi MHD, Poortmans F, Hamers R, et al. Crystal structure of a camel single-domain V-H antibody fragment in complex with lysozyme. *Nat Struct Biol* 1996;3:803–11.
- Holliger P, Hudson PJ. Engineered antibody fragments and the rise of single domains. *Nat Biotechnol* 2005;23:1126–36.
- Muyldermans S, Cambillau C, Wyns L. Recognition of antigens by single domain antibody fragments: the superfluous luxury of paired domains. *Trends Biochem Sci* 2001;26:230–5.
- Rasmussen SGF, Choi H-J, Fung JJ, Pardon E, Casarosa P, Chae PS, et al. Structure of a nanobody-stabilized active state of the beta(2) adrenoceptor. *Nature* 2011;469:175–80.
- Goldman ER, Anderson GP, Conway J, Sherwood LJ, Fech M, Vo B, et al. Thermostable llama single domain antibodies for detection of botulinum A neurotoxin complex. *Anal Chem* 2008;80:8583–91.
- Kirchofer A, Helma J, Schmidthals K, Frauer C, Cui S, Karcher A, et al. Modulation of protein properties in living cells using nanobodies. *Nat Struct Mol Biol* 2010;17:133–62.
- Rothbauer U, Zolghadr K, Muyldermans S, Schepers A, Cardoso MC, Leonhardt H. A versatile nanotrap for biochemical and functional studies with fluorescent fusion proteins. *Mol Cell Proteomics* 2008;7:282–9.
- Rothbauer U, Zolghadr K, Tillib S, Nowak D, Schermelleh L, Gahl A, et al. Targeting and tracing antigens in live cells with fluorescent nanobodies. *Nat Methods* 2006;3:887–9.
- Fridy PC, Li Y, Keegan S, Thompson MK, Nudelman I, Scheid JF, et al. A robust pipeline for rapid production of versatile nanobody repertoires. *Nat Methods* 2014;11:1253–60.
- Zhang Y, Yu X, Hou L, Chen J, Li P, Qiao X, et al. CTA1: purified and display onto gram-positive enhancer matrix (GEM) particles as mucosal adjuvant. *Protein Expres Purif* 2018;141:19–24.
- Li L, Qiao X, Chen J, Zhang Y, Zheng Q, Hou J. Surface-displayed porcine reproductive and respiratory syndrome virus from cell culture onto gram-positive enhancer matrix particles. *J Ind Microbiol Biot* 2018;45:889–98.
- Yang PC, Chu RM, Chung WB, Sung HT. Epidemiological characteristics and financial costs of the 1997 foot-and-mouth disease epidemic in Taiwan. *Vet Rec* 1999;145:731–4.

- [32] Bachrach HL, Trautman R, Breese Jr SS. Chemical physical properties of virtually pure foot-and-mouth disease virus. *Am J Vet Res* 1964;25:333–42.
- [33] Harmsen MM, Seago J, Perez E, Charleston B, Eble PL, Dekker A. Isolation of single-domain antibody fragments that preferentially detect intact (146S) particles of foot-and-mouth disease virus for use in vaccine quality control. *Front Immunol* 2017;8:960.
- [34] Zhang J, Zhu C, Fan D. Endotoxin removal from recombinant human-like collagen preparations by Triton X-114 two-phase extraction. *Biotechnol* 2013;12:135–9.
- [35] Bolden JS, Warburton RE, Phelan R, Murphy M, Smith KR, De Felippis MR, et al. Endotoxin recovery using limulus ameocyte lysate (LAL) assay. *Biologicals* 2016;44:434–40.
- [36] Correa W, Brandenburg K, Zaehring U, Ravuri K, Khan T, von Wintzingerode F. Biophysical analysis of lipopolysaccharide formulations for an understanding of the low endotoxin recovery (LER) phenomenon. *Int J Mol Sci* 2017;18:2737.
- [37] Li H, Yang Y, Zhang Y, Zhang S, Zhao Q, Zhu Y, et al. A hydrophobic interaction chromatography strategy for purification of inactivated foot-and-mouth disease virus. *Protein Express Purif* 2015;113:23–9.
- [38] Yang Y, Li H, Li Z, Zhang Y, Zhang S, Chen Y, et al. Size-exclusion HPLC provides a simple, rapid, and versatile alternative method for quality control of vaccines by characterizing the assembly of antigens. *Vaccine* 2015;33:1143–50.
- [39] Announcement No. 2078 of Ministry of Agriculture and Rural Affairs of the People's Republic of China. [http://www.moa.gov.cn/nybggb/2014/dsiq/201712/t20171219\\_6110301.htm](http://www.moa.gov.cn/nybggb/2014/dsiq/201712/t20171219_6110301.htm) [accessed 1 December 2018].
- [40] Fry EE, Stuart DJ, Rowlands DJ. The structure of foot-and-mouth disease virus. *Curr Top Microbiol Immunol* 2005;288:71–101.
- [41] Kabat E, Wu HM, Perry TT, Gottesman KS, Foeller C. Sequence of proteins of immunological interest. US Department of Health and Human Services, U.S. Public Health Service, NIH Bethesda, MD.1991; 91: 3242.
- [42] Vu KB, Ghahroudi MA, Wyns L, Muylldermans S. Comparison of llama VH sequences from conventional and heavy chain antibodies. *Mol Immunol* 1997;34:1121–31.
- [43] Acharya R, Fry E, Stuart D, Fox G, Rowlands D, Brown F. The three-dimensional structure of foot-and-mouth-disease virus at 2.9 Å resolution. *Nature* 1989;337:709–16.
- [44] Wild TF, Brown F. Nature of the inactivating action of trypsin on foot-and-mouth disease virus. *J Gen Virol* 1967;1:247–50.
- [45] De Genst E, Silence K, Decanniere K, Conrath K, Loris R, Kinne R, et al. Molecular basis for the preferential cleft recognition by dromedary heavy-chain antibodies. *Proc Natl Acad Sci USA* 2006;103:4586–91.
- [46] Skerra A, Pluckthun A. Assembly of a functional immunoglobulin Fv fragment in escherichia-coli. *Science* 1988;240:1038–41.
- [47] Thanongsakrrikul J, Srimanote P, Maneewatch S, Choowongkamon K, Tapchaisri P, Makino S-i, et al. A VHH that neutralizes the Zinc metalloproteinase activity of botulinum neurotoxin type A. *J Biol Chem* 2010;285:9657–66.
- [48] Wang D, Yang S, Yin S, Shang Y, Du P, Guo J, et al. Characterization of single-domain antibodies against Foot and Mouth Disease Virus (FMDV) serotype O from a camelid and imaging of FMDV in baby hamster kidney-21 cells with single-domain antibody-quantum dots probes. *BMC Vet Res* 2015;11:120.
- [49] Yin S, Yang S, Shang Y, Sun S, Zhou G, Jin Y, et al. Characterization of Asia 1 sdAb from camels bactrianus (*C. bactrianus*) and conjugation with quantum dots for imaging FMDV in BHK-21 cells. *PLoS One* 2013;8(5):e63500.
- [50] Monegal A, Ami D, Martinelli C, Huang H, Aliprandi M, Capasso P, et al. Immunological applications of single-domain llama recombinant antibodies isolated from a naive library. *Protein Eng Des Sel* 2009;22:273–80.
- [51] Harmsen MM, van Solt CB, Fijten HPD, van Keulen L, Rosalia RA, Weerdmeester K, et al. Single-domain antibody fragments against foot-and-mouth disease. *Vet Microbiol* 2007;120:193–206.